UDK: 629.7.051.5 :533.6.071.3
COSATI: 01-03, 01-01

Increasing Launch Capability of a UAV Bungee Catapult

Zoran Novaković[1)]
Nikola Medar[1)]
Lidija Mitrović[1)]

In this paper, a concept of a UAV (Unmanned Aerial Vehicle) bungee catapult is analyzed by introducing an appropriate combination of elastic and non elastic cords which significantly increases efficiency (by decreasing of power losses) compared to a widely spread concept of a bungee catapult with elastic cords only. This enables installing a few times greater number of elastic bungee cords into the same modular space in the bungee catapult. The concept of elastic and non elastic cords gives the bungee catapult a possibility to hand over to a UAV more than twice greater launch energy in relation to the concept of elastic cords only. Also, in the paper, a mathematical model of a UAV new bungee catapult with elastic and non elastic cords is given, as well as the analysis comparing the energy losses of both concepts.

Key words: **UAV, launching, launching device, catapult, design, mathematical model**.

Nomenclature

x – distance, absolute cord elongation
$\dot{x}, v$ – UAV-launch trolley velocity
v_F – final velocity of UAV- launch trolley
t_F – final time-duration of the launching phase
$\ddot{x}, a$ – acceleration
α – launching rail elevation angle
R_z, R_x – force of lift, force of drag
q – stiffness of the fictive elastic cord
b_0 – cord length (non-elongated)
Δx – cord elongation
L – effective rail-launching length
m_{UAV} – mass of the Unmanned Aircraft Vehicle
m_{LT} – mass of the cradle
μ – static friction coefficient
N – inclined plane perpendicular reaction
T – UAV propulsive force
F_e – force of the fictive elastic cord
F_μ – frictional sliding force
$t_0, \dot{x}_0, x_0$ – initial values of the differential equation
A_g – gravitational force work
$A_{\mu 1,2,3}$ – frictional sliding force work
A_c – effective elastic cord force work
A_{CR} – real elastic cord force work
A_T – propulsive force work
F_{er} – force of the real elastic cord
A – aerodynamic surface of the wing
n – number of cords
S – reaction force of the rope
t_k – time when the launch trolley stops
ϕ, ψ – angular position of the traveling pulley
$\dot{\phi}, \dot{\psi}$ – angular velocity of the traveling pulley
R, r – radius of rollers
F_{BR} – breaking force
C_x – drag force coefficient
C_z – lift force coefficient
β – angle between the launch rail and the rope
d – catapult design characteristic
T_0 – propeller thrust when the UAV is at rest
E_k – UAV-launch trolley kinetic energy

Introdustion

PREVIOUS benchmark analyses [3, 4] have shown that UAV bungee catapults have advantages compared to their competitors (pneumatic, hydraulic, kinetic energy, Rocket Assisted Takeoff - RATO catapults) concerning simplicity of their construction, low purchase cost and maintenance cost. The main disadvantages of UAV bungee catapults are a limited capability to launch greater mass with a required launch speed, and a significant gradient of acceleration change on the launching rail ("jerk" action). In a widespread conception of UAV bungee catapults [2], Fig.3, elastic cords are not only a power source, but also a part of the driving system of the catapult, since they pull the launch trolley directly [2], Fig. The driving system consists of the launch trolley and a set of bungee cords and rollers, over which the bungees are rewound when changing their direction of motion. The mathematical model that describes the driving system of the catapult [2] is valid with a number of constraints (assumptions) and it gives theoretical results. By assumptions setting, most of the energy loss is neglected. This requires an adoption of elastic cords with a greater energy capacity compared to the theoretical results in order to compensate for neglected losses.

Increasing the power capacity of the UAV bungee catapult [2] could be achieved either by a selection of

[1)] Military Technical Institute (VTI), Ratka Resanovića 1, 11132 Belgrade, SERBIA

stronger elastic cords (increasing the elastic cord cross section) or by increasing the number of elastic cords. However, increasing the elastic cord cross section demands increasing the minimum roller radius over which the elastic cord is enwrapped, while increasing the elastic cords number demands the increase of the width of the rollers over which the elastic cords are arranged. In both variants, the mass of rollers increases considerably, which brings in additional inertia into the catapult driving system, leading to the decrease of efficiency. At the same time, the enlargement of the rollers width (the number of cords) is limited by the acceptable launch ramp overall dimensions and by the design constraints.

All of this leads to the conclusion that the power capacity increase of the UAV bungee catapult [2] is practically limited. The existing UAV bungee catapults [2], (Israeli bungee catapults for UAV Skylark II, Sparow, etc.) indicate that the number of installed elastic cords is not bigger than six. Considering current producers of bungees in accordance with aeronautical standards, it could be noticed that the technology of bungee cords is significantly improved [14]. Analogously to the calculation of the bungee catapult concept [2], a theoretical result is achieved that (within the range of 20% to 80% of cord elongation) six elastic cords Ø30 [14] installed into the catapult ([2], Fig.3) can deliver the effective work of 47500J. The actual energy that this catapult concept [2] can deliver to the UAV is substantially lower, and the losses can be determined by experimental trials only. For the expected actual efficiency ratio 0.7 of the catapult, the actual delivered kinetic energy is 33kJ, which matches the launch energy of a mass of 70kg with a launch speed of ~30m/s.

The actual delivered kinetic energy of the UAV bungee catapult [2] imposes the need for increasing its launch capability in order to achieve a potential of pneumatic and hydraulic catapults. The concept of the UAV bungee catapult described in [2] is limited concerning the increase of its actual launching capabilities, higher than 33kJ. The solution can be found in the catapult concept modification. It is the concept of the UAV bungee catapult which introduces a combination of elastic cords and a non-elastic cord (a multi-strand steel rope, or a rope).

Design Task Setup of a New Concept of the Bungee Catapult

Generally, the bungee catapult main task is to hand over to the UAV previously accumulated energy in elastic cords so that the UAV, at the time of leaving the catapult, has a speed of at least 15% greater than the stall speed for a given configuration of the UAV. To have a successful takeoff, the UAV should have sufficient lift force after the instant of leaving the catapult when its own driving propeller achieves stable flight take over.

According to the selected functional scheme, for the adopted necessary elastic cord stiffness, it is required to define the effective launching rail length, so that the required takeoff speed of the UAV is feasible and that the acceleration is less than 10g.

Also, from the new concept of the UAV bungee catapult, a significant increase of the launch capabilities and power loss decrease are required. Essentially, power loss is mainly a result of great inertia into the catapult system [2] and the irregular operating of elastic cords enwrapping the rollers with changing movement directions of cords, which considerably degrades its energetic performance [2].

Functional scheme of the New Concept of the Bungee Catapult

The concept of the UAV bungee catapult with elastic and non elastic cords, Fig.1, is considered as a material system made of a stationary catapult body - launching ramp (1), and a dynamic system. Besides a launch trolley (2) with a UAV (10) and a double set of elastic cords (5), the dynamic system comprises a tension rope – a non elastic cord (6), connected to the launch trolley over the pulley system by one of its ends. By its other end, the rope is spooled onto the drum of the electric winch (3). The front side of the elastic cords set is connected to the back side of the slider (4). On the front of its side, the slider carries the freerotating travelling pulley (7), over which the tension rope is rewound. The rear side of the elastic cords set is fixed to the rear side of the launching ramp frame. The stationary freerotating pulleys (8 and 9) have a role of the rotating support during the rewinding of the tension rope over them. The launching ramp can be designed in a stationary version or more often in a mobile version when it is mounted on a trailer or a truck. The catapult body design enables an adjustable setup launching rail elevation angle (α=7°÷20°).

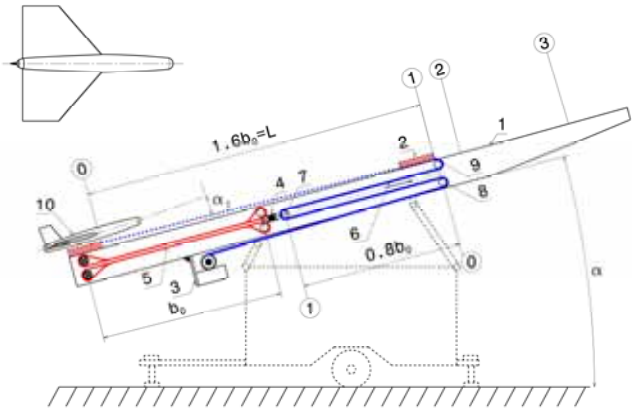

Figure 1. Functional scheme of the UAV bungee catapult

One can notice that massive rollers, which rewind a full set of elastic cords ([2], Fig.2), are replaced here with small mass pulleys, over which a tension rope is rewound. The elastic cords lay free and operate at one plane now, enabling their contraction without any losses except hysteresis. The change of a movement direction is now taken over by the tension rope, which is rewound over negliglible inertia pulleys. It enables a significant increase of the catapult power capacity, by choosing stronger elastic cords (enlarging of the cord cross-section), as well as by increasing the number of elastic cords (elastic powerband contains maximum twenty cords). Elastic cords are densely packed next to each other, which requires minimum modular space.

The new concept UAV bungee catapult does not include a damper that stops the launch trolley after the UAV takeoff, as applied in the case of the concept in [2] (Fig.2). Here, after the UAV takeoff, the oscillatory motion of the launch trolley (back and forth - around its final equilibrium position) is stopped by the friction brake, the mechanism of which is activated by opening the launch trolley, when the UAV leaves. This requires a significant extension of the launch ramp in relation to the concept in[2](Fig.2).

Description of the dynamic system

The catapult is ready for launching when the launch trolley is in its start position (0) on the launch rail, while the traveling pulley slider, located opposite to the launch trolley, is simultaneously in its (0) position. In the position (0), a double

set of elastic cords is tensioned to the maximum, 80% of its free length b_0. The launch trolley is started from the rest by pulling the safety pin. The elastic cords are pulled backwards dragging the slider with the traveling pulley, which pulls the rope with the launch trolley. The electric winch drum is blocked during the launching phase so it cannot rewind the rope. When pulling the elastic cords back, and moving the launch trolley forwards, the rope is rewound over the stationary pulley (9) and the traveling pulley (7), equally distributed simultaneously to the both sides of the pulley (7). At the same time, the pulley (8) does not rotate because the winch drum is blocked. When the launch trolley passes the effective launching distance $1.6b_0$ and arrives to its position (1), the elastic cords are contracted completely for a length of $0.8b_0$ (view in Fig.1), when the traveling pulley slider reaches its position (1). The rope with the length of $1.6b_0$, which was on the top of the launching rail when the launch trolley was in its position (1), is rewound and is distributed to the double length of $0.8b_0$ on the both sides of the traveling pulley (7).

In position (1), the launch speed is greatest, but in that moment the launch trolley is still not open for the reasons of protection of elastic cords from damage. Namely, if the UAV is released in position (1), the catapult dynamic system rapidly loses great UAV mass at the critical moment, when elastic cords are entirely relieved. This would lead to undesirable, uncontrolled vibrations of the elastic cords, causing their damage. Therefore, the launch trolley with the UAV is allowed to continue the movement inertially, to move some distance and get in position (2) when the trolley opens and releases the UAV.

Since the launch trolley with the UAV continues to move inertially from position (1) to position (2), the elastic cords instantly pass from the contraction phase to the extension phase and begin to slow down the launch trolley with the UAV. Reaching position (2), the launch trolley loses its speed slightly and the launch trolley opening mechanism starts to release the UAV.

With the opening of the launch trolley and the UAV takeoff, the catapult dynamic system instantly loses significant weight, which leads to a rapid increase in speed, acceleration and amplitude of the launch trolley oscillation on the launching rail. Therefore, with the launch trolley opening, the friction sliding brake is started simultaneously, which, together with the elastic cords at the phase of extension, slows down the launch trolley additionally.

After releasing the UAV, the launch trolley from position (2) continues its retarded motion to position (3), when the speed drops to zero. The launch trolley achieves the maximum amplitude in position (3) and changes the movement direction. The stretched elastic cords now retreat back the launch trolley indirectly through the rope to position (1), when the cords are relieved again. The launch trolley continues its movement inertially, and extends the elastic cords again to a new equilibrium position when the speed drops to zero, changes its direction of movement, etc. The friction sliding forces of the brake and the trolley act as damping to the catapult dynamic system, so that the launch trolley stops entirely after a few full oscillations around position (1).

In order to set the launch trolley in its start position (0) again, it is necessary to unblock the electric winch drum to rotate freely and to close the launch trolley to disconnect the brake. Then, the launch trolley is backed down manually, from its stop position (1) to its start position (0), and is locked by the safety pin. Thereby, the rope is absolutely free to be unwound from the electric winch drum for a length of $1.6b_0$.

To re-tense the double set of elastic cords for the length of $0.8b_0$ and to prepare the catapult to re-launch, it is necessary to clutch the drum to the electric winch. By starting the electric winch, the rope over the pulleys (7 and 8) is wound onto the drum where the elastic cords are tensioned. At the same time, the traveling pulley slider moves from its position (1) to position (0) for a length of $0.8b_0$. The rope is on the drum for a length of $1.6b_0$ which was unwound from the drum when the launching cradle was manually repositioned from position (1) to position (0). When the electric winch drum is blocked, the catapult is ready to relaunch the UAV.

Mathematical model

In order to determine the law of motion on the launching rail, the differential equations of motion of the catapult dynamic (material) system are suitable to be formulated by using D'Alambert principle. For this purpose, the connections are cut (disconnected), and the reactions of the connections are introduced instead, i.e. at each point of the dynamic system inertial forces are added.

The result of the consideration of the following assumptions represents a simplification of the working forces in the bungee catapult dynamic system (Fig.2).

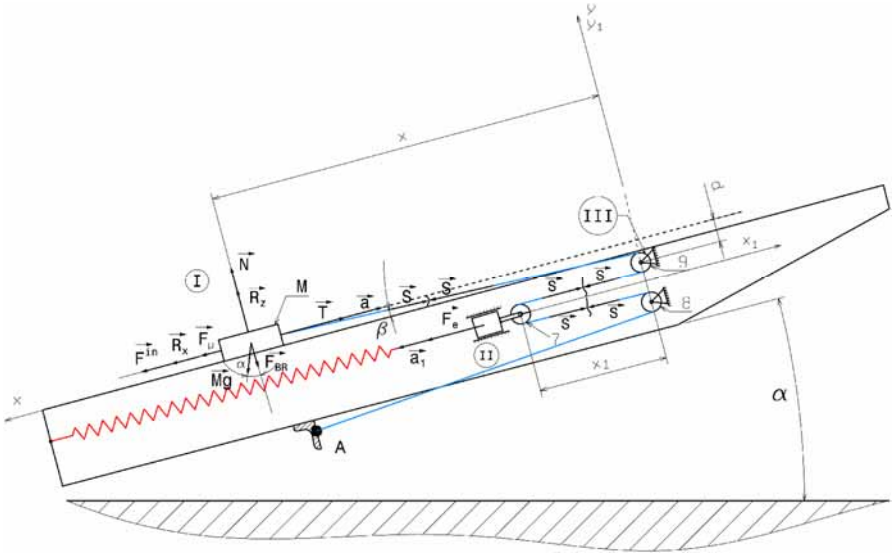

Figure 2. Free bodies diagram of the dynamic system of the catapult

Assumption 1.
- *The catapult dynamic system is considered as the kinetics of a system of rigid bodies [6].*

Assumption 2.
- *The mass of the elastic cords is neglected.*

Assumption 3.
- *The masses of the non-elastic cord, the pulleys (7,8 and 9, Fig.1) and the slider are neglected.*

Assumption 4.
- *Acting forces onto the dynamic system are coplanar.*

Assumption 5.
- *Friction forces in bearings are neglected.*

Assumption 6.
- *The force Rz is collinear to N, i. e. they act perpendicularly to the inclined plane.*

In order to achieve sufficient lift force, the UAV is set up onto the launch trolley at the angle α_1 to the inclined plane. Since the angle α_1 is relatively small ($\cos\alpha_1 \sim 1$) this assumption can be adopted as correct.

Assumption 7.
- *It is considered that the UAV propeller pulling force T is constant.*

This assumption is taken into consideration in order to simplify equation (35). The value of T decreases with speed increase. It is assumed that the average constant value T performs the same work as the real T.

Assumption 8.
- *It is considered that the rope is absolutely un-stretchable and flexible and that the rope rewinding, over pulleys, is performed without slipping.*

The sum of all external forces-***Q***-(active forces and reactions of connections) and inertial forces-***in***, of the catapult dynamic system is equal to zero, which can be represented in a general form ([7, 8]):

$$\sum_{i=1}^{n} \vec{F}_i^{Q,in} = 0 \tag{1}$$

The sum of the moments of all external and inertial forces of the catapult dynamic system that exert in respect to the fixed pole O is equal to zero, which can be represented in a general form ([7], [8]):

$$\sum_{i=1}^{n} \vec{M}_o^{\vec{F}_i^{Q,in}} = 0 \tag{2}$$

As a result of cutting the connections in the catapult dynamic system, three free units are obtained: the launch trolley with the UAV, as (I), the traveling pulley slider, as (II) and the stationary pulley (9), as (III), Fig.2. The catapult dynamic system possesses one degree of freedom. The stationary pulley (8) is motionless (rotate resting) all the time, since one end of the rope is connected to the blocked electric winch drum (the fixed point A). Besides the coordinate system Oxy, the coordinate system Ox_1y_1 is introduced additionally in order to define a relation of movement between the launch trolley with the UAV and the travelling pulley slider. The analysis of the relation of movement, i.e. the relation between the coordinates x and x_1 is shown in Fig.3.

When the traveling pulley slider (7), upon acting of the force F_e is displaced linearly for the infinitesimal amount dx_1, the pulley (7) is rotated for the infinitesimal angle $d\psi$ at the same time, since one end of the rope is connected to the fixed point A. The traveling pulley linear displacement for dx_1 and the rope rewinding over it for the lenght $Rd\psi$ causes the pulley (9) rotating for the infinitesimal angle $d\varphi$, by which the rope is rewound over the same pulley for the lenght $rd\varphi$ to the traveling pulley. This leads to the linear displacement of the launch trolley for the amount dl, including the rope distribution for the lenght $(dl)_1$ and $(dl)_2$ of both sides of the traveling pulley (7). Supposing that all previous statements are valid, it is possible to form the following relations:

$$dl = \left(\frac{dl}{2}\right)_1 + \left(\frac{dl}{2}\right)_2 \tag{3}$$

$$\left(\frac{dl}{2}\right)_1 = dx_1 \tag{4}$$

$$\left(\frac{dl}{2}\right)_2 = Rd\psi \tag{5}$$

$$dx \cong dl = rd\phi \tag{6}$$

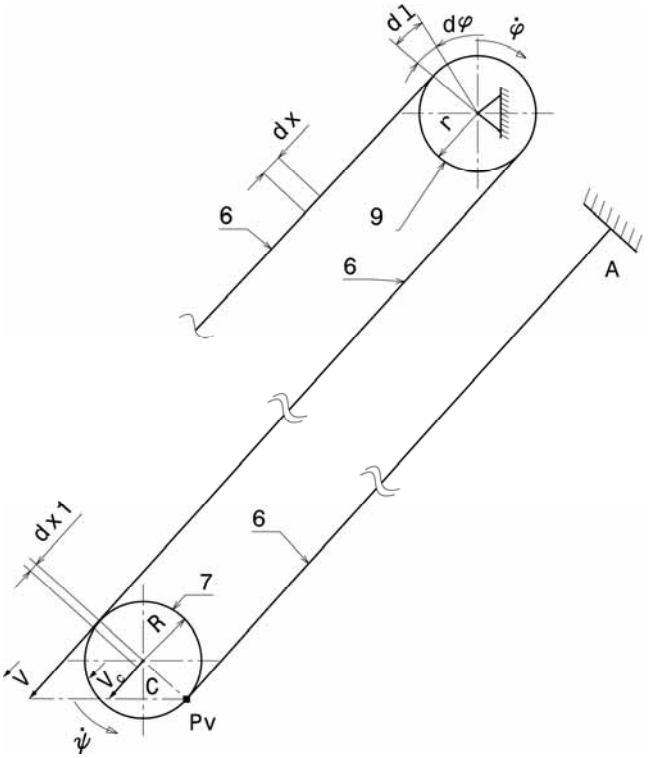

Figure 3. Travelling pulley kinematic scheme

Since the traveling pulley performs translation and rotation (planar motion), the instantaneous zero velocity pole is situated at the point P_v. From the velocity plan layout, the following relation can be established:

$$\upsilon_c = \frac{\upsilon}{2} \tag{7}$$

Also, from the velocity level is:

$$\upsilon = r\dot{\phi} = 2R\dot{\psi} \tag{8}$$

so it follows:

$$\dot{\psi} = \frac{r}{2R}\dot{\phi} \tag{9}$$

That is for $r=R$

$$\dot{\psi} = \frac{1}{2}\dot{\phi} \tag{10}$$

From equations (10) and (6) it follows:

$$dx_1 = \frac{1}{2} r d\phi = \frac{1}{2} dl = \frac{1}{2} dx \tag{11}$$

By integration equation (11) is obtained:

$$x_1 = \frac{1}{2} x + c, c = 0$$

and finally

$$x_1 = \frac{1}{2} x\,. \tag{12}$$

Equation (12) represents the displacement of the traveling pulley slider with respect to the displacement of the launch trolley with the UAV when the traveling pulley (7) and the stationary pulley (9) are of the same diameter.

In order to retain the same rewinding length of the rope over the stationary pulley (8) and the same dispalcement of the travelling pulley slider (7), at the electric winch drum operation, it is necessary that the pulley (8) and the pulleys (7) and (9) have the same diameter.

Applaying equation (1) in the scalar form to unit (I), Fig.2, the next two equations are obtained:

$$\sum_{i=1}^{n} X_i^{Q,in} = F^{in} + R_x + F_\mu + Mg \cdot \sin\alpha - T - S \cdot \cos\beta = 0 \tag{13}$$

$$\sum_{i=1}^{n} Y_i^{Q,in} = N + R_x - Mg \cdot \cos\alpha - S \cdot \sin\beta - (F_{BR}) = 0 \tag{14}$$

If equation (1) is applied in the scalar form to unit (II), the next equation is obtained:

$$\sum_{i=1}^{n} X_i^{Q,in} = S + S - F_e \tag{15}$$

The inertial force of the launch trolley with the UAV is:

$$F^{in} = -M\ddot{x} \tag{16}$$

The mass of the launch trolley with the UAV is:

$$M = m_{LT} + m_{UAV} \tag{17}$$

The UAV drag force is:

$$R_X = C_X \frac{\rho \cdot \dot{x}^2}{2} A \tag{18}$$

The sliding friction force of the trolley onto the launching rail is:

$$F_\mu = -\mu \cdot N sign(\dot{x}) \tag{19}$$

The UAV propeller pulling force [7] is:

$$T = T_0 \left(1 - \frac{\dot{x}}{\upsilon_S}\right) \cong T(\dot{x}) \tag{20}$$

The angle β between the launching rail and the rope (the force S) is changeable, and it is the smallest at the launch trolley start position (0) while it grows with the launch trolley moving to the pulley (9), when it achieves its maximum amount of 90° (see Fig.2).

From Fig.2 $\sin\beta = \frac{d}{\sqrt{x^2 + d^2}}$, that is $\cos\beta = \frac{x}{\sqrt{x^2 + d^2}}$, where d is a catapult design characteristic.

The UAV lift force is:

$$R_Z = C_Z \frac{\rho \cdot \dot{x}^2}{2} A \tag{21}$$

The reaction of the brake perpendicular to the inclined plane is:

$$(F_{BR}) = const \tag{22}$$

The brake starts acting after the launch trolley is opened. The time of the launch trolley opening is negligible.

Assumption 9.

- *The work of the friction force when the UAV slips off the cradle (at the end position) is neglected.*

The work of the friction force when the UAV slips off the cradle is comparatively small due to a short run distance.

The inclined plane (launching rail) reaction N is obtained from equation (14):

$$N = Mg \cdot \cos\alpha + S \cdot \frac{x}{\sqrt{x^2 + d^2}} - R_X - (F_{BR}) \tag{23}$$

The rope reaction S is obtained from equation (15). The effect of assumption 3 is constant amount of the rope reaction at rewinding over the pulleys.

$$S = \frac{1}{2} F_e \tag{24}$$

The term of the sliding friction force assumes finally the following form:

$$F_\mu = -\mu \left[Mg \cos\alpha + \frac{F_e}{2} \frac{x}{\sqrt{x^2 + d^2}} - C_x \frac{\rho x^2}{2} A + (F_{BR}) \right] sign\dot{x} \tag{25}$$

In general, from the static characteristic diagram of a real bungee cord, one cord force as a function of absolute elongation (the coordinate x_1) can be obtained in the form:

$$F_e^1 = a_3 x_1^3 + a_2 x_1^2 + a_1 x_1 \tag{26}$$

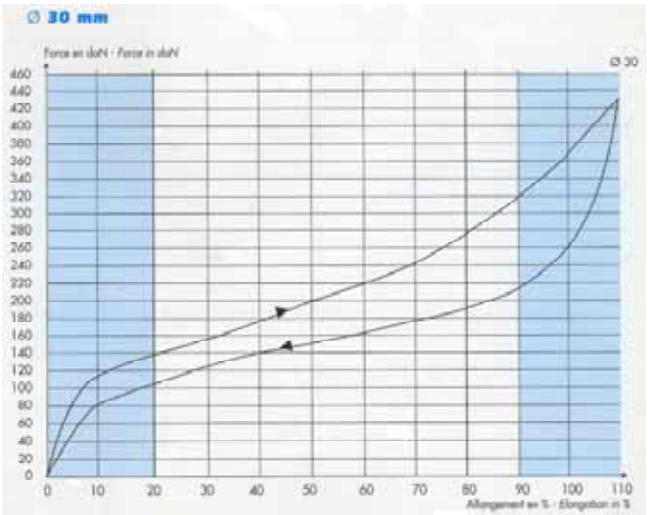

Figure 4. Force/Elongation diagram of a Ø30mm real bungee cord [14]

The force of the total number n of the installed elastic cords in the catapult (double set cords) is:

$$F_e = n\left(a_3 x_1^3 + a_2 x_1^2 + a_1 x_1\right) \tag{27}$$

By introducing relation (12) in expression (27), it is obtained:

$$F_e = n\left[a_3\left(\frac{x}{2}\right)^3 + a_2\left(\frac{x}{2}\right)^2 + a_1\left(\frac{x}{2}\right)\right] \tag{28}$$

Since larger diameters of real bungee cords are characterized by hysteresis (Fig.4) that could not be neglected, then the force of elastic cords as a function of the launch trolley displacement can be formulated:

$$F_e = \begin{cases} \frac{na_3}{8}x^3 + \frac{na_2}{4}x^2 + \frac{na_1}{2}x \ , x > 0 \\ \frac{na_{33}}{8}x^3 + \frac{na_{22}}{4}x^2 + \frac{na_{11}}{2}x \ , x < 0 \end{cases} \tag{29}$$

where the coefficients a_1, a_2 and a_3 are related to the lower curve, while the coefficients a_{11}, a_{22} and a_{33} are related to the upper curve. At the launch trolley acceleration, the elastic cords deliver energy to the catapult according to the lower curve, Fig.4.

From equation (13), it is obtained:

$$S = \frac{1}{\cos\beta}\left(F^{in} + F_\mu + R_X + Mg\sin\alpha - T\right) \tag{30}$$

When equation (30) is applied to (15), it is obtained:

$$F_e - \frac{2}{\cos\beta}\left(F^{in} + F_\mu + R_X + Mg\cdot\sin\alpha - T\right) = 0 \tag{31}$$

By introducing expressions (16, 18, 25) in (31), the differential equation of motion onto the catapult launching rail is obtained:

$$\begin{aligned} \ddot{x} = {} & \frac{C_X\rho A + \mu C_z \rho A\cdot sign(\dot{x})}{2M}\cdot\dot{x}^2 - \\ & -\left(\frac{|x|}{2M\sqrt{x^2+d^2}} + \frac{\mu\cdot d}{2M\sqrt{x^2+d^2}}\right)F_e - \frac{T}{M} - \\ & -\mu g\cdot\cos\alpha\cdot sign(\dot{x}) + g\cdot\sin\alpha - \\ & -\left(\frac{\mu F_{BR}}{m_{LT}}\cdot sign(\dot{x})\right) \end{aligned} \tag{32}$$

Equation (32), which comprises equation (29), is a non-linear and non-homogeneous second order ordinary differential equation (ODE) that can be solved by the numerical method of integration. The applicable method is based on the explicit Runge-Kutta (4, 5) formula and the Dormand-Prince method, ([10, 12]) by which the MATLAB solver "ode45" operates. Since this method can only solve the first order ODE, the above is converted to two first order ODEs as follows. The new state variables x_2 and x_3 are introduced with the following derivation:

$$x_2 = x, \quad x_3 = \dot{x} \tag{33}$$

If the first derivative is applied in (33), the following is obtained:

$$\dot{x}_2 = \dot{x}, \quad \dot{x}_3 = \ddot{x} \tag{34}$$

After substituting (32) in (34), it gives two new first order ODEs, which are:

$$\begin{aligned} \dot{x}_2 = {} & x_3, \\ \dot{x}_3 = {} & \frac{C_X\rho A + \mu C_Z\rho A\cdot sign(x_3)}{2M}\cdot x_3^2 - \\ & -\left(\frac{|x_2|}{2M\sqrt{x_2^2+d^2}} + \frac{\mu\cdot d}{2M\sqrt{x_2^2+d^2}}\right)\cdot \\ & \cdot\left(\begin{cases} \frac{na_3}{8}x_2^3 + \frac{na_2^2}{4}x_2^2 + \frac{na_1}{2}x_2 \ , x_2 > 0 \\ \frac{na_{33}}{8}x_2^3 + \frac{na_{22}}{4}x_2^2 + \frac{na_{11}}{2}x_2 \ , x_2 < 0 \end{cases}\right) - \\ & -\frac{T}{M} - \mu g\cdot\cos\alpha\cdot sign(x_3) + g\cdot\sin\alpha - \\ & -\left(\frac{\mu F_{BR}}{m_{LT}}\cdot sign(x_3)\right) \end{aligned} \tag{35}$$

Numerical example

According to the selected functional schema (Fig. 1), and the mathematical model, the design characteristics (F_e, M, F_{BR}) are varied into (35) in order to fulfill all the requirements of the design task set up of the new Conception of the bungee catapult and to find the best launch capabilities of the New Catapult, which are related to the launch mass and the launch speed.

Since this catapult is designed for the launch of so-called "tandem"-configuration UAVs (reconnaissance UAVs) which requires slightly lower launch speed, and for the launch of "delta"-configuration UAVs (aerial target UAVs) that requires some higher launch speed, the demand can be set for a launch speed of 30m/s.

Using representative points along the curves (Fig.4) of the adopted cord, real data values input vectors for the lower curve and the upper curve are formed. At the same time, the transformation of the relative elongation into the absolute elongation (within the range from 0% to 110% elongation of the "un-stretched" cord length, b_0=5m) is performed. The frst column represents the absolute cord elongation x_1 in (m), and the second column represents the one cord force F_e^1, in (N).

$$data := \begin{bmatrix} 0 & 0 \\ 0.11 & 234.41 \\ 0.23 & 433.26 \\ 0.37 & 653.36 \\ 0.49 & 781.08 \\ 0.74 & 894.22 \\ 1.03 & 1000.16 \\ 1.29 & 1106.16 \\ 1.56 & 1190.82 \\ 1.78 & 1268.47 \\ 2.05 & 1338.92 \\ 2.31 & 1388.02 \\ 2.55 & 1437.19 \\ 2.8 & 1493.44 \\ 3.05 & 1556.8 \\ 3.3 & 1627.27 \\ 3.54 & 1697.78 \\ 3.79 & 1754.03 \\ 4.04 & 1824.5 \\ 4.3 & 1923.4 \\ 4.54 & 2043.68 \\ 4.8 & 2249.27 \\ 5.02 & 2490.51 \\ 5.2 & 2824.33 \\ 5.35 & 3286.22 \\ 5.5 & 4110.86 \end{bmatrix}$$

lower curve

$$data1 := \begin{bmatrix} 0 & 0 \\ 0.09 & 376.72 \\ 0.2 & 703.59 \\ 0.38 & 1008.94 \\ 0.49 & 1086.9 \\ 0.73 & 1207.19 \\ 1.03 & 1320.21 \\ 1.28 & 1404.9 \\ 1.55 & 1489.55 \\ 1.79 & 1588.51 \\ 2.05 & 1687.41 \\ 2.32 & 1814.72 \\ 2.55 & 1913.7 \\ 2.8 & 1998.4 \\ 3.06 & 2097.31 \\ 3.29 & 2196.26 \\ 3.54 & 2323.65 \\ 3.79 & 2472.36 \\ 4.04 & 2635.3 \\ 4.27 & 2819.6 \\ 4.54 & 3053.62 \\ 4.78 & 3273.47 \\ 5.01 & 3514.7 \\ 5.25 & 3812.8 \\ 5.5 & 4110.86 \end{bmatrix}$$

upper curve

For the model function

$$y(x_1) = a_3x_1^3 + a_2x_1^2 + a_3x_1 \tag{36}$$

according to expressions (26) and (29), the fitted function is obtained in the form:

$$F_e^1 = \begin{cases} F^1(x_1) = 81.032x_1^3 - 617.95x_1^2 + 1609x_1, lower\ \ curve \\ G^1(x_1) = 67.707x_1^3 - 546.449x_1^2 + 1735x_1, upper\ \ curve \end{cases} \tag{37}$$

Plotting the data points and the fitted function (37) gives the graph:

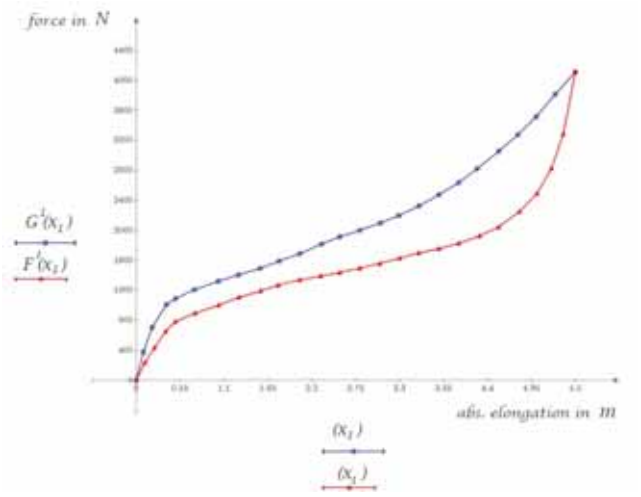

Figure 5. Fitted curve of the adopted Ø30 real bungee cord

The linear combination of the data is acceptable fit to the data. This is confirmed by the values of the correlation coefficients for both curves, which are close to 1.

$$corr\left(F^1(x_1), F^1\right) = 0.99$$
$$corr\left(G^1(x_1), G^1\right) = 0.98 \tag{38}$$

The use of twenty Ø30 real bungee cords is the highest possible installed energy into the catapult. The summable twenty Ø30 real bungee cords maximum force is:

$$F_e = n \cdot F_e^1 = 20 \cdot \begin{cases} F^1_{(x_1=4)} = 36480N \\ G^1_{(x_1=4)} = 52700N \end{cases} \tag{39}$$

One real bungee cord effective work is:

$$A_C^1 = \int_0^4 F^1(x_1) \cdot dx_1 \cong 4872J \text{ , for the lower curve} \tag{40}$$

For the double set of bungee cords, the effective work is:

$$A_C = 20 \cdot A_C^1 = 97449J \tag{41}$$

For the varied values (F_e, M, F_{BR}):

F_e - defined by equation (39) and (40)

F_{BR}=4000N

$M=m_{UAV}+m_{LT}$=175+20=195kg

and the adopted Design Characteristics:

$b_{max}=0.8 \cdot b_0=0.8 \cdot 5$=4m

(b must satisfy bungee cord producer recommendations)

μ=0.1

α=15° (0.2186rad)

T=250N

C_x=0.4

C_z=0.05

ρ=1.225m^3/kg

A=2.9m^2

n=20

d=0.25m,

and the initial values:

$$t_0=0s,\ x(0)=8m \tag{42}$$

numerical integration of (35), in the MATLAB software by using the solver "ode45", gives the solution in the form of the following graphs:

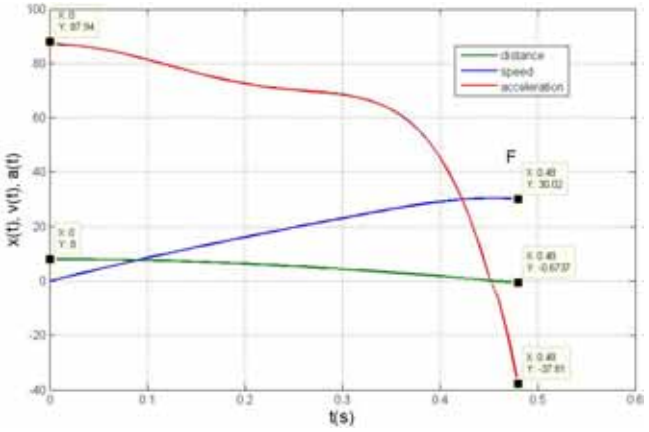

Figure 6. Distance-Speed-Acceleration Diagram until the instant UAV takeoff

The end point of each curve (Fig.6) is the instant, t_F=0.48s when the UAV takes off. For the UAV mass of 175kg, the takeoff speed is v_F=30m/s. The UAV is exposed to the maximum acceleration of 9g at the start point.

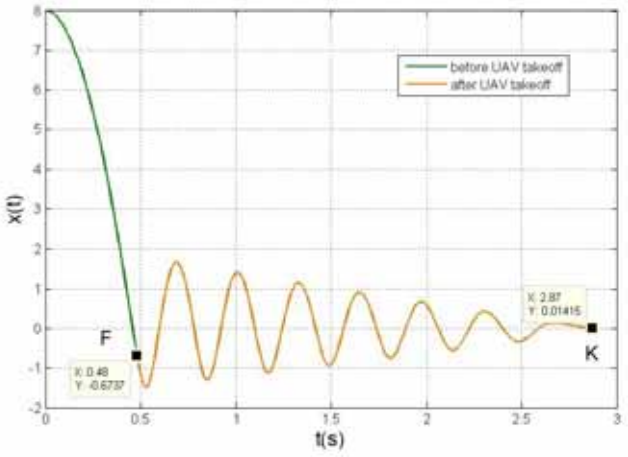

Figure 7. Cumulative changes of the distance on the launching rail

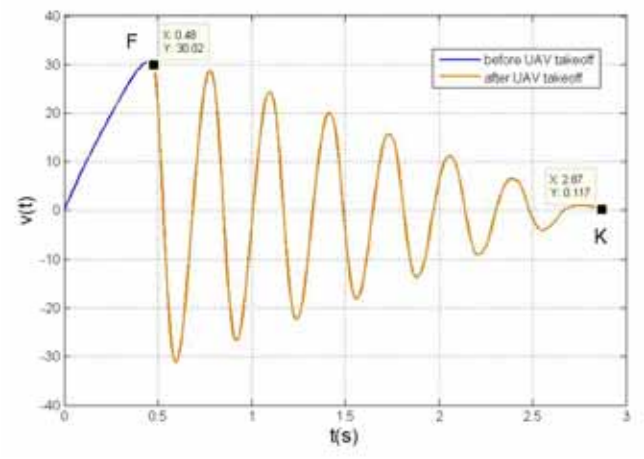

Figure 8. Cumulative changes of the speed on the launching rail

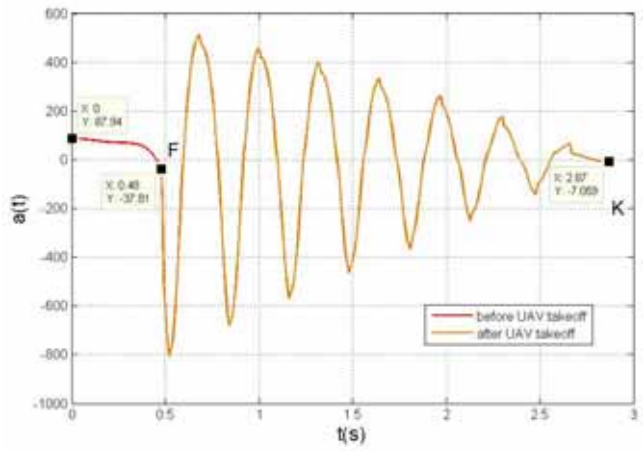

Figure 9. Cumulative changes of the acceleration on the launching rail

Figures 7-9, represent the cumulative changes of distance, speed and acceleration on the catapult launching rail, from the initial moment t_0 to the last moment t_K, when the launch trolley stops. At the instant $t_F = 0.48\text{s}$, when the launch trolley is opened and the UAV takes off, the sliding frictional brake simultaneously starts acting by force of 4000N which slows down additionally the launch trolley, until the launch trolley is at rest by $t_k = 2.87\text{s}$. The changes of the characteristic of speed and acceleration at the instant t_F can be noticed, since the catapult dynamic system loses significant weight and due to influence of the frictional brake. It can be concluded from Fig.7 that the minimum effective length of the launching rail for the adopted and varied values in this numerical example is 9m.

Results verification

The verification of the results ($v_F = 30\,\text{m/s}$, $m_{UAV} = 175\,\text{kg}$) can be done by means of the work kinetic energy theorem.

$$E_{K_F} - E_{K_0} = \sum_i A_i \tag{43}$$

The elastic cords and the UAV propulsion enter effective work into the bungee catapult. The elastic cords effective work A_C is:

$$A_C = n \cdot A_C^1 = 20 \cdot \left(\int_0^4 f(x_1)\,dx_1 - \int_0^{\frac{0.6737}{2}} g(x_1)dx_1 \right) = 95635\text{J} \tag{44}$$

The UAV propulsion effective work A_T is:

$$A_T = T \cdot (1.6b_0 + 0.6737) = \\ = 250 \cdot (1.6 \cdot 5 + 0.6737) = 2168.5\text{J} \tag{45}$$

The elastic cords and the UAV propulsion effective work is converted to the UAV and the launch trolley kinetic energy E_{KF}, and wasted to the gravitational force work of the UAV and the launch trolley A_g, to the frictional sliding force work A_μ, and to the work of the UAV force drag A_{Rx}.

$$E_{KF} = \frac{M}{2} \cdot \upsilon_F^2 = \frac{195 \cdot 30^2}{2} = 87750J \tag{46}$$

$$A_g = Mg\left(y - y_0\right) = Mg \cdot (1.6b_0 + 0.6737) \cdot \sin\alpha = \\ = 195 \cdot 9.81 \cdot 8.6737 \cdot \sin(15^\circ) = 4294.4J \tag{47}$$

Since the brake does not act at the launching phase, and F_{BR}=0 in equation (25), the frictional sliding force work can be presented as:

$$A_\mu = A_{\mu 1} + A_{\mu 2} + A_{\mu 3} \tag{48}$$

where:

$$A_{\mu 1} = \mu Mg \cos\alpha \cdot (1.6 \cdot b_0 + 0.6737) = 1602\text{J} \tag{49}$$

$$A_{\mu 2} = -\int_0^{8.6737} \frac{\mu C_Z \rho A}{2} \cdot \dot{x}^2 dx \tag{50}$$

By introducing the following change in equation (50):

$$dx = \dot{x}dt \tag{51}$$

equation (52) is obtained. The solver "ode45" calculates $x(t)$ and $\dot{x}(t)$ for each step of integration and delivers their value output vectors. Integrals (52), and (54) are numerically calculated in MATLAB by using the solver "trapz" where $x(t)$ and $\dot{x}(t)$ value vectors are used as an input, so that

$$A_{\mu 2} = -\int_0^{0.48} \frac{\mu C_Z \rho A}{2} \cdot \dot{x}^3 dt = -45J \tag{52}$$

$$A_{\mu 3} = \mu \cdot \int_0^{8.6737} \frac{F_e}{2} \cdot \frac{x}{\sqrt{x^2 + d^2}} dx = \mu \cdot \\ \cdot \int_0^{8.6737} \left(\begin{cases} f(x_1 = \frac{x}{2}), x > 0 \\ g(x_1 = \frac{x}{2}), x < 0 \end{cases} \right) \cdot \frac{x}{2\sqrt{x^2 + d^2}} dx \tag{53}$$

When the substitution of (51) in (53) is introduced, it is obtained:

$$A_{\mu 3} = \mu \cdot \int_0^{0.48} \left(\begin{cases} \frac{a_3}{8} x^3 + \frac{a_2^2}{4} x^2 + \frac{a_1}{2} x \ , x > 0 \\ \frac{a_{33}}{8} x^3 + \frac{a_{22}}{4} x^2 + \frac{a_{11}}{2} x \ , x < 0 \end{cases} \right) \cdot \frac{\dot{x} \cdot x}{2\sqrt{x^2 + d^2}} dt \quad (54)$$

By the numerical integration in MATLAB, it is obtained

$$A_{\mu 3} = 123.1J \quad (55)$$

so that from expression (48), it is obtained:

$$A_{\mu} = 1680J \quad (56)$$

The work of the UAV drag force is:

$$A_{R_X} = \int_0^{8.6737} \frac{C_X \rho A}{2} \dot{x}^2 \cdot dx = \int_0^{0.48} \frac{C_X \rho A}{2} \dot{x}^3 \cdot dt = 3583\text{J} \quad (57)$$

The final result is:

$$A_C + A_T \cong E_{KF} + A_g + A_{\mu} + A_{R_X} \quad (58)$$
$$(97803.5\text{J}) > (97307.4\text{J})$$

with the error less than 0.51%, so the calculation could be accepted as correct.

Conclusion

The calculated catapult efficiency, i.e. the calculated efficiency ratio can be defined as the ratio between the catapult delivered energy to the launch trolley with the UAV and the effective work which is entered into the catapult by the elastic cords and the propulsion of the UAV.

$$\eta = \frac{E_{KF}}{A_C + A_T} = \frac{87750}{95635 + 2168.5} = 0.897 \Rightarrow 90\% \quad (59)$$

The loss of energy of ~10% is spent on performing works A_{μ}, A_g and A_{Rx}. The actual catapult efficiency ratio is:

$$\eta_R = \frac{E_{KFr}}{A_C + A_T} \quad (60)$$

where E_{KFr} is the actual kinetic energy that the catapult delivers to the launch trolley with the UAV at the launching phase.

Additional losses in the catapult which are not introduced in the calculation are the consequence of the introduced assumptions. The most influential is assumption 2, i.e. assumption 3. Practically, it can be adopted that by introducing assumption 3, the summable mass of 20kg is neglected, which corresponds to the mass of the launch trolley. In the first approximation, the energy loss of this neglected mass corresponds to the gravity work of the launch trolley (406J from equation (47), which degrades the calculated efficiency ratio η by 0.4%. By introducing assumption 2, the neglected mass is considerably bigger (~200kg, for twenty bungees of Ø30mm in diameter), but this effect to the dynamic catapult system can only be determined experimentally. Finally, if the additional loss of energy of 4000J is adopted, then E_{KFr}=83750J, the catapult with the actual efficiency ratio η_R=0.86 would be able to launch the UAV with a mass of 165kg and a speed of v_F=30m/s.

References

[1] Jane's.: *Unmanned Aerial Vehicles and Targets*, Issue 29, 2007, Launch and Recovery Chapter.

[2] NOVAKOVIĆ,Z., MEDAR,N.: *Analysis of a UAV Bungee Cord Launching Device*, Scientific Technical Review, ISSN 1820-0206, 2013, Vol.63, No.3, pp.41-47.

[3] RAYMER,D.P.: *Aircraft Design: A Conceptual Approach*, 4th ed., AIAA Education Series, AIAA Virginia, 2006.

[4] FRANCIS,J.: *Launch System for Unmanned Aerial Vehicles for use on RAN Patrol Boats*, Final Thesis Report 2010, SEIT, UNSW@ADFA

[5] MCDONNELL,W,R.: *United States patent application publication, Launch and recovery system for unmanned aerial vehicles*, 2006, URL: http://www.freepatentsonline.com/7097137.html [accessed on 5 September 2010]

[6] HIBBELER,R.C.: *Engineering Mechanics Dynamics*, 2nd ed., Prentice Hall, Singapore, 2004, Chaps. 12, 14.

[7] МЕЩЕРСКИЙ,И.В.: *Сборник задач по теоретической механике*, Москва 1986, 36-издание

[8] BATJ,M.I., DZENALIDZE,G.J., KELZON,A.S.: *Rešeni zadaci iz teorijske mehanike sa izvodima iz teorije*, Dinamika II, Prevod sa ruskog, Građevinska knjiga, Beograd, 1972

[9] FEHLBERG,E.: *Low-order Classical Runge-Kutta Formulas with Stepsize Control*, NASA Technical Report R-315, 1969.

[10] LAMBERT,J.D.: *Computational methods on Orinary ODEs*, John Wiley and Sons, New York, p278,1973

[11] ERWIN,K.O.: *Runge Kutta Runge Kutta Nyastrom Method for direct solution of second order ODEs*, Advanced Engineering Maths, 8th Edition, John Wiley and sons Inc. p958-961, New Delhi, 1999.

[12] KIMURA,T.: *On Dormand-Prince Method*, September 24,2009

[13] http://reference.wolfram.com/mathematica/tutorial/NDSolveExplicitRungeKutta.html

[14] "Sandow Technic" catalogue of bungee cords, www.sandowtechnic.com

Received: 30.12.2014.

Povećanje lansirne moći bandži katapulta

U ovom radu se analizira koncepcija bandži katapulta za bespilitne letelice sa primenom odgovarajuće kombinacije elastičnih i neelastičnih užadi čime se značajno povećava efikasnost (smanjenjem gubitaka) u odnosu na široko rasprostranjenu koncepciju bandži katapulta samo sa elastičnim užadima. Istovremeno se u katapultu, u istom smeštajnom prostoru, omogućava instalisanje nekoliko puta većeg broja elastičnih užadi što značajno povećava lansirnu moć katapulta. Sve to, koncepciji bandži katapulta sa elastičnim i neelastičnim užadima, daje mogućnost da preda bespilotnoj letelici više od dva puta veću energiju lansiranja u odnosu na koncepciju bandži katapulta samo sa elastičnim užadima. U radu je dat matematički model nove koncepcije bandži katapulta sa elastičnim i neelastičnim užadima i uporedna analiza energetskih gubitaka obe koncepcije.

Ključne reči: **bespilotne letelice, lansiranje, lansirni uređaj, katapult, projektovanje, matematički model.**

Увеличение мощности запуска банджи-катапульта

В этой статье проанализирована концерция банджи-катапульта для беспилотных летательных аппаратов с помощью соответствующей комбинации упругих и неупругих канатов, что значительно увеличивает эффективность (снижением потерь), в связи с широко распространённой концепции банджи-катапульта только с упругими канатами. В то же время в катапульте, в том же пространстве хранения, позволена установка в несколько раз большего количества упругих канатов, что значительно увеличивает силу катапульта со момента его запуска. Всё это, концепции банджи-катапульта с упругими и неупругими канатами, обеспечивает способность передать беспилотному летательному аппарату более чем в два раза больше энергии запуска по отношению к концепции банджи-катапульта только с упругими канатами. В статье представлена и математическая модель новой концепции банджи-катапульта с упругими и неупругими канатами и сравнительный анализ потерь энергии в обеих концепциях.

Ключевые слова: **беспилотные летательные аппараты (БЛА), запуск, пусковое устройство, катапульт, дизайн, математическая модель.**

Augmentation de capacité de lancement chez la catapulte "bungee"

Dans ce travail on analyse la conception de catapulte "bungee" pour les aéronefs sans pilote avec l'emploi de la combinaison convenable des cordes élastiques et non élastiques ce qui augmente considérablement l'efficacité (diminuant les pertes) par rapport à la conception très rependue de catapulte "bungee" possédant seulement les cordes élastiques. En même temps on permet à cette catapulte dans le même espace l'installation d'un nombre de cordes élastiques plusieurs fois plus grand ce qui augment significativement la capacité de lancement de catapulte. Tout cela donne la possibilité à la conception de catapulte "bungee" avec les cordes élastiques ou non élastiques de fournir à l'aéronef sans pilote l'énergie de lancement deux fois plus grande que chez la catapulte possédant seulement les cordes élastiques. On a présenté aussi le modèle mathématique de la nouvelle conception de catapulte "bungee" avec les cordes élastiques et non élastiques ainsi que l'analyse comparée des pertes énergétiques pour les deux conceptions.

Mots clés: **aéronefs sans pilote, lancement, dispositif de lancement, catapulte, conception, modèle mathématique.**